Properties of fluorine-doped tin oxide films produced by atmospheric pressure chemical vapor deposition from tetramethyltin, bromotrifluoromethane and oxygen

James Proscia* and Roy G. Gordon
Department of Chemistry, Harvard University, Cambridge, MA 02138 (USA)

(Received April 2, 1991; revised December 16, 1991; accepted January 20, 1992)

Abstract

Fluorine-doped tin oxide films were produced by atmospheric pressure chemical vapor deposition from various mixtures of tetramethyltin, bromotrifluoromethane, and oxygen. Growth rates of up to 60 nm s^{-1} were achieved. Optical measurements to assess the visible transparency are presented. Hall effect measurements revealed mobilities of up to 42 $cm^2 V^{-1} s^{-1}$ and carrier concentrations typically in the range $(1-6) \times 10^{20}$ cm^{-3}. Microprobe analysis revealed the presence of electrically inactive fluorine atoms especially at low deposition temperatures and at high tetramethyltin (2 mol.%) and bromotrifluoromethane (4 mol.%) compositions. However, at high deposition temperature and low tetramethyltin (0.5 mol.%) or low bromotrifluoromethane (0.5 mol.%) mixtures, almost all the fluorine dopant atoms are electrically active. Scanning electron microscopy studies revealed an increase in surface texturing when the tetramethyltin concentration was decreased or the oxygen concentration was increased. X-ray crystallography showed preferential orientation of the crystallites for most reaction conditions.

1. Introduction

Transparent conducting thin films are important materials in the fabrication of heat reflecting (*i.e.* low *E*) windows and as transparent surface electrodes in thin film solar cells, liquid crystal displays, and electrochromic devices. Tin oxide doped with either antimony or fluorine has become an important material used in these applications. The properties of tin oxide films have been previously reviewed by Jarzebski and Marton [1–3] and transparent conductors by Chopra *et al.* [4]. Tin oxide films have been produced by a number of techniques such as spray pyrolysis [5–12], the sol–gel technique [13], reactive r.f. sputtering [14], and atmospheric pressure chemical vapor deposition (APCVD) [15–18].

The evaporation and sputtering techniques tend to produce films at low growth rates on the order of 0.1 nm s^{-1}. Of the processes used to produce doped tin oxide films, spray pyrolysis and APCVD are most well suited for the large area, high volume deposition of tin oxide coated glass and solar cells. Both methods are capable of depositing material with high growth rates on the order of 10–100 nm s^{-1}. In the spray pyrolysis technique [5–12], an aqueous and/or alcoholic solution containing a suitable tin compound (such as tin tetrachloride or monobutyltin trichloride) and a suitable dopant (*i.e.* antimony trichloride, hydrofluoric acid, ammonium fluoride) is atomized and directed onto a heated substrate upon which a tin oxide film is subsequently deposited. The method is restricted by the fact that film surface uniformity is affected by the size distribution of the spray droplets, the temperature of the substrate [5], and the requirement that the spray nozzle be continuously moved along a substrate if good film thickness uniformity is to be achieved. Impingement of large liquid droplets on the glass leads to local cooling, creating a spotty thickness non-uniformity referred to as mottle. Spray pyrolysis is capable of producing doped tin oxide films with good electrical and optical properties [6, 7]. In the APCVD process, film uniformity is determined by the uniformity with which the reactant gases are dispersed and by the temperature uniformity of the substrate. The droplet size is obviously not a consideration.

Tin oxide is a semiconductor which is made conductive by n-type dopants which fall into two categories: (1) pentavalent metals such as antimony which substitute for tin atoms, and (2) halogens such as fluorine or chlorine which replace oxygen. The choice of dopant can be guided by understanding that tin oxide is a fairly ionic compound for which the metal orbitals dominantly form the conduction band, while the oxygen orbitals make up most of the filled valence band.

*Present address: Ford Motor Company, Dearborn, MI 48120, USA.

0040-6090/92/$5.00

Substituting a metal for tin induces a large local perturbation in the conduction band, frequently scattering the electrons in the conduction band. This reduces the mobility of the electrons, which subsequently degrades the conductivity and transparency of the material. A halogen substituting for oxygen, however, mainly disturbs the filled valence band, and only slightly disturbs the electrons in the conduction band. Chlorine and the heavier halogens are so large that they distort the lattice and cause additional electron scattering. Of the halogens, fluorine causes the least scattering, and fluorine doping leads to tin oxide films with the highest conductivity and transparency [4, 8, 17]. In either type of substitution, a positively charged scattering center is produced [19].

The oxidation of tetramethyltin to produce tin oxide was first described by Baliga and Ghandhi [16]. Fluorine doping in tin oxide through the decomposition of fluorocarbons was discovered by Gordon [17]. More recently, the APCVD reaction of tetramethyltin (TMT), bromotrifluoromethane (a Freon), and oxygen was analyzed by Borman and Gordon [18]. In the present paper, the material properties of fluorine-doped tin oxide produced by APCVD from TMT, bromotrifluoromethane, and oxygen will be presented. This APCVD process is capable of growing tin oxide films at high growth rates with values of up to 60 nm s^{-1} achieved in the present study. Conditions are found in which nearly 100% of the fluorine dopant atoms are electrically active. It will be shown that this material has excellent electrical properties as illustrated by a high d.c. conductivity and Hall mobility, as well as a high visible transmittance. Crystal orientation, fluorine atom concentration, and surface structure are investigated and related to the quality of the films produced.

2. Experimental details

2.1. Description of the atmospheric pressure chemical vapor deposition apparatus

Fluorine-doped tin oxide films were produced by passing various mixtures of TMT, oxygen, and bromotrifluoromethane (a Freon) into a heated reaction zone as illustrated in Fig. 1. Stock mixtures of TMT and bromotrifluoromethane were prepared from technical grade TMT and a standard mixture of the Freon in air (purchased from Matheson Gas Products). The TMT had a purity of about 97% with the major impurities being hydrocarbons and ethers. By preparing a few stock mixtures of TMT, Freon and air, the concentrations of the reactants could be varied over a reasonable range with gas flowmeter tubes. For some of the depositions, the desired amount of Freon was established by using pure bromotrifluoromethane (purity, better than 99.7%).

The reaction chamber was constructed as follows: a 2.5 cm thick nickel plate is placed on top of a large laboratory hot plate which provides most of the heat for the APCVD reactions. A heating tape is placed around the edges of the nickel plate in order to provide some auxiliary heating control. The heating tape is controlled by an RFL controller with a thermocouple probe embedded in the plate. A piece of heat-insulating material, 0.7 cm thick and cut in the shape of a U, is placed over this metal plate. Resting on this is a nickel block with a row of entrance holes which distribute the reactant gas mixture. The actual reaction zone consists of a bottom wall formed by the nickel plate on which the substrates rest, three side walls defined by the heat-insulating material, and an upper wall consisting of the nickel block. The missing fourth side of the U-shaped insulation provides an exhaust for the reaction gases and ensures that the deposition occurs at 1 atm pressure. In addition, the missing fourth side provides an opening through which the sample substrates can be introduced. An important feature of this reactor is that the upper metal block is air cooled, causing the top surface of the reaction chamber to be at a lower temperature than the substrate. This temperature gradient causes powder (gas phase nucleation products) to be levitated away from the substrate by thermophoresis.

Corning 7059 glass plates (10 cm by 10 cm) were used as substrates in the present study. After the substrates are passed into the reaction chamber they are allowed to come to thermal equilibrium. The surface temperature of the substrates is measured prior to deposition by an Ircon optical pyrometer through a hole in the top metal block. The hole is then plugged during the deposition. Linear flow velocities were typically about 60 cm s^{-1}. The reaction gas flow is essentially laminar with a Reynolds' number of approximately 10.

2.2. Methods for evaluating film properties

Specular transmission and reflection were measured on a Varian 2390 spectrophotometer. Diffuse transmission and reflection were measured on a Perkin–Elmer 330 spectrophotometer equipped with an integrating sphere detector. The integrating sphere ensures that any scattered light will not be mistakenly attributed to absorption in the film. In solar cell applications, the diffuse component is desirable. It is related to the phenomenon of light trapping which increases the efficiency of amorphous silicon solar cells [20, 21].

The sheet resistance of the tin oxide films was measured with a Veeco four-point probe. The sheet resistance was converted to a conductivity by measuring the thickness of the film. The conductivity is related to the

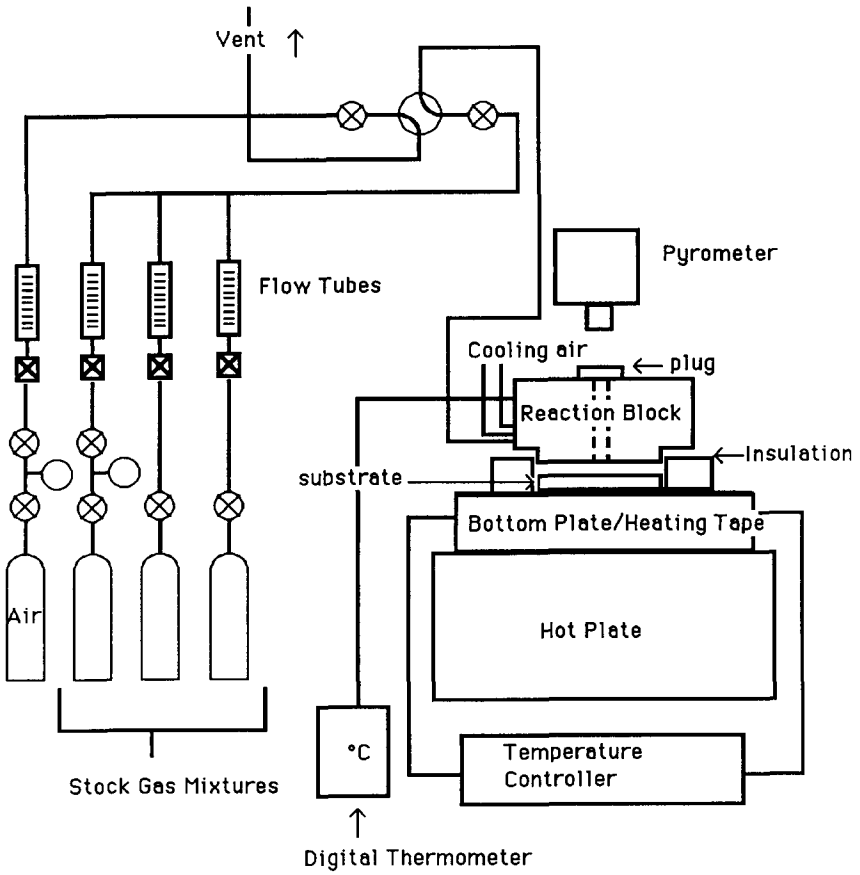

Fig. 1. Schematic diagram of the APCVD system used to deposit fluorine-doped tin oxide from TMT and Freon.

sheet resistance by $\sigma = 1/Rd$, where σ is the conductivity, R is the sheet resistance, and d the film thickness. Thicknesses were determined by a stylus profilometer (Dektak), or through analysis of interference fringes in the reflectance spectrum, or by counting interference fringes under monochromatic light (546 nm) and interpolating for points in between. Film thicknesses less than 120 nm were measured on a Rudolph Research ellipsometer. Most of the films were approximately 1 μm thick. The films were further analyzed by measuring the Hall effect. This allows determination of the carrier concentration and electron mobility when the thickness and sheet resistance are known.

Microprobe and Auger analyses for fluorine concentration were carried out to determine the fluorine atom concentration in the films. The microprobe analysis was performed on a Cameca MBX microprobe and the Auger analysis on a Perkin–Elmer Thin Film Analyzer (model 540A). Calcium fluoride was used as the reference for fluorine and a tin oxide crystal (cassiterite) was the reference for tin in the microprobe analysis. The reference samples were coated with a thin carbon film in order to make them conductive. The fluorine-doped tin oxide films were also coated with a carbon film of approximately the same thickness. The tin oxide films were sufficiently thick that penetration of the electron beam to the substrate was not a complication in the microprobe analysis. Determination of the fluorine atom concentration combined with the Hall effect measurements allowed us to obtain the doping efficiency, *i.e.* the fraction of the fluorine atoms in the film actually contributing electrons to the conduction band. It is not possible to measure the tin atom and fluorine atom concentrations to sufficient accuracy to rule out the occurrence of a slight amount of oxygen deficiency in the films. Oxygen vacancies would contribute to the free electron density. However, a tin oxide film deposited at 570 °C from 2.0 mol.% TMT in air (no Freon present) had a conductivity over 1000 times lower than a typical fluorine-doped film. This implies that oxygen vacancies do not make a significant contribution to the free electron concentration in the present CVD process.

Surface morphology was investigated by scanning electron microscopy (SEM) on a JEOL JSM 35U microscope. X-ray diffraction studies were performed on a Philips powder X-ray diffractometer. From the X-ray data the crystallite orientation and sizes were deter-

mined [22]. A copper target ($\lambda = 0.154$ nm) was used as the X-ray source.

3. Results

3.1. Film composition

It was found that the tin dioxide films produced were stoichiometric in tin to oxygen to the degree of accuracy of both Auger and microprobe analysis. Further, the Auger analysis did not reveal the presence of either carbon or bromine, two other elements present in the reacting gases. The Auger analysis for fluorine was not quantitative because of electron-induced desorption of fluorine (requires films to be sputtered while analyzed), and lack of suitable calibration standards. Therefore, no further Auger results will be presented. Microprobe analysis probes more of the bulk of the film and is therefore not as susceptible to electron-induced fluorine desorption. All the fluorine atom concentrations discussed below were determined by microprobe analysis.

3.2. Flow directional dependence of film properties

In the APCVD system described above the substrate is stationary with the reacting gases flowing directly above it. Because of this there is typically a gradient in thickness along the flow direction. Films deposited at temperatures of 520 °C and below had peak thicknesses late in the flow, while films grown at 570 °C and above were found to peak early in the flow. Figure 2 is a plot of the film thickness variation along the flow direction for films grown at 440 °C and 570 °C with a concentration of 2.0 mol.% TMT, 4 mol.% Freon, and balance air (19 mol.% oxygen, 75 mol.% nitrogen). At the lower temperatures the film thickness builds up along the flow while at higher temperatures the films are thicker at the beginning of the flow. At low temperatures the gas phase chemical reactions limit the rate of film production with the amount of reaction increasing along the flow direction, reaching a maximum and then decreasing. However, at higher temperatures the gas reactions occur very rapidly and the rate of film growth becomes diffusion limited. Therefore most of the film is deposited early with the gas phase reactants becoming depleted further along the flow direction. Similar thickness profiles have been observed in other APCVD studies [18, 23, 24]. Peak growth rate is defined as the film growth rate at that point along the flow direction where the maximum film thickness occurs.

In a static reactor, the gas phase chemistry will change along the flow direction because reactants become depleted and converted to chemical intermediates and products. This changing chemistry can cause the properties of the tin oxide films to change along the flow direction. Figure 3 is a plot of the film conductivity and Hall mobility *vs.* position along the flow for a film grown at 610 °C with a 1.0 mol.% TMT concentration, 2 mol.% Freon, and balance air (approximately 19 mol.% oxygen, 78 mol.% nitrogen). The mobility and conductivity are nearly constant along the flow direction. Figure 4 gives the carrier concentrations and total fluorine atom concentrations for this film along the flow. Early in the deposition the carrier concentration is nearly equal to the fluorine atom concentration. Thus the doping efficiency (the ratio of the number of carriers to the number of fluorine atoms) is unity. Along the flow the fluorine atom concentration increases slightly and then appears to remain constant. The carrier concentration does not fully track this effect and does not rise quite as much in the middle and late flow regions. For many of the films produced at higher temperatures by our APCVD process, fluorine atom concentration increased by a greater amount than carrier concentration. In this specific example, the accumulation of electrically inactive fluorine atoms did not have a detrimental effect on the electrical properties as suggested

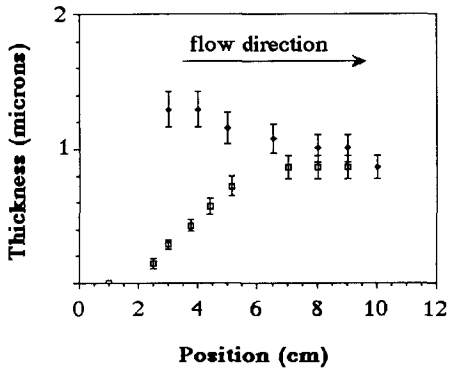

Fig. 2. Variation in the tin oxide thickness along the flow direction at 440 °C (□) and 570 °C (◆). The input flow rates are 3.0 l min^{-1} and 4.5 l min^{-1} respectively.

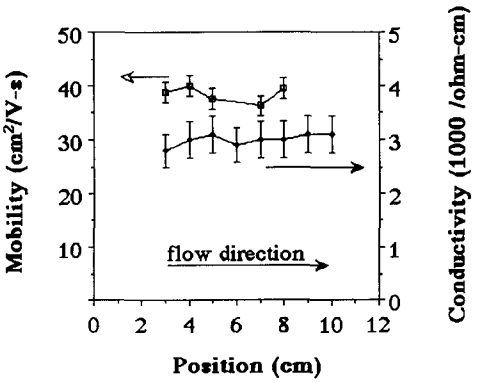

Fig. 3. Conductivity and Hall mobility for a film along the flow direction for a film grown at 1 mol.% TMT, 2 mol.% Freon in air at 610 °C.

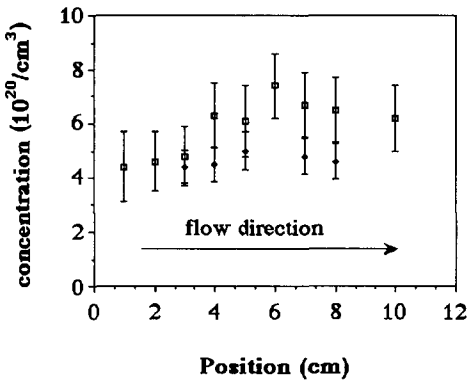

Fig. 4. Variation in carrier concentration (◆) and fluorine atom concentration (□) along the flow direction for a film grown at 0.5 mol.% TMT, 1 mol.% Freon in air at 610 °C.

by the fairly constant mobility. Other conditions will be presented below in which there is a large excess of inactive fluorine atoms. In those cases, the large excess of inactive fluorine may be limiting the quality of the films.

3.3. *Film properties as a function of thickness*

The electrical properties of tin oxide films as a function of film thickness were investigated. Tin oxide films were grown by the previously outlined APCVD process from a vapor mixture containing a TMT concentration of 1.0 mol.%, a Freon concentration of 4 mol.%, and a balance of air (19 mol.% oxygen, 76 mol.% nitrogen); Corning 7059 glass substrates at a temperature of 570 °C were used. These conditions have been shown to produce high quality tin oxide films [25].

Tin oxide films produced by other methods tend to show a significant increase in conductivity as the thickness is increased [26, 27]. Figure 5 contains a plot of film conductivity *vs.* film thickness. The conductivity is lower for very thin films. Films approximately 60 nm thick have only about one-half the conductivity of thick films. However, the conductivity quickly improves by a film thickness of 0.25 μm to about 80% of its value at 1 μm. The low conductivity of very thin films may be due to the initial formation of smaller loosely packed crystallites at the beginning of film growth [28]. As the film is allowed to grow thicker the crystallites should become larger and more densely packed, thereby improving the film quality by reducing the scattering from grain boundaries. Thinner films may also be more susceptible to the effects of carriers scattering from the film surface because of the higher surface to volume ratio. Figure 5 also provides a plot of the apparent crystallite size (from X-ray line widths) *vs.* film thickness. The size is nearly constant from 0.14 to 1 μm. The X-ray scans for films with thicknesses between 0.14 and 1 μm revealed that films grown under these conditions are highly oriented along the (200) direction. The peak growth rate of the films in this series was found to be approximately 23 nm s^{-1} and independent of film thickness.

Figure 6 is a plot of both sheet resistance and maximum transmission *vs.* film thickness. The maximum transmission is the absolute maximum value in the spectral transmission spectrum occurring at an interference maximum. This value usually occurs around a wavelength of 600 nm. The maximum transmission for a non-absorbing film should be about 90%, with the 10% loss resulting from reflection. Figure 6 should be useful in choosing a film thickness to achieve various combinations of sheet resistance and transmission properties to be used in the design of a solar cell. For example, if a sheet resistance of 20 Ω/□ can be tolerated in a small solar cell, a peak transmission of almost 90% can be achieved. However, for a large commercial panel, a sheet resistance of 5 Ω/□ may be desirable; in this case, we would expect a value of 84% for the transmission. In general, the combination of transmission and sheet resistance attainable with this method is excellent. A more detailed analysis of the visible absorption properties of the tin oxide films will be presented in a subsequent paper.

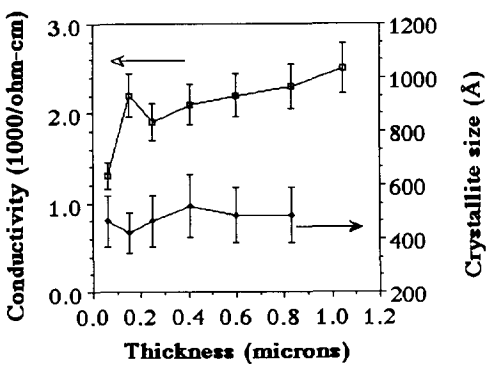

Fig. 5. Variation in conductivity (□) and crystallite size (◆) as a function of thickness for films grown at 1 mol.% TMT and 4 mol.% Freon in air at 570 °C.

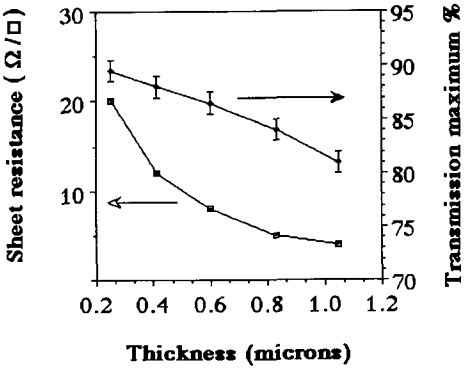

Fig. 6. Dependence of the maximum transmission and sheet resistance as a function of thickness for films grown at 1 mol.% TMT and 4 mol.% Freon in air at 570 °C.

3.4. Film growth rate

In high volume industrial coating applications, the film growth rate is a very important parameter. High values are desirable if good quality films can also be produced. Figure 7 shows an increase in peak film growth rate as a function of substrate temperature. At low temperatures of 440 °C the deposition is very slow with a maximum rate of 3 nm s^{-1} while at the higher temperatures values of nearly 60 nm s^{-1} are achieved.

Figure 8 gives the growth rates at 570 °C for tin oxide films grown at TMT concentrations of 0.1, 0.5, 1.0, and 2.0 mol.% as a function of Freon concentration. In general, the growth rate is higher at higher TMT concentration with a peak value of 56 nm s^{-1} at 2 mol.% TMT and 4 mol.% Freon. At TMT concentrations below about 1 mol.%, the growth rate does not appear to depend on the Freon concentration, while at TMT concentrations of 1 mol.% and higher the Freon has a slight accelerating effect with the growth rates somewhat higher at the higher Freon levels.

The growth rate was observed to increase initially and then to level off as the oxygen concentration increased (Fig. 9).

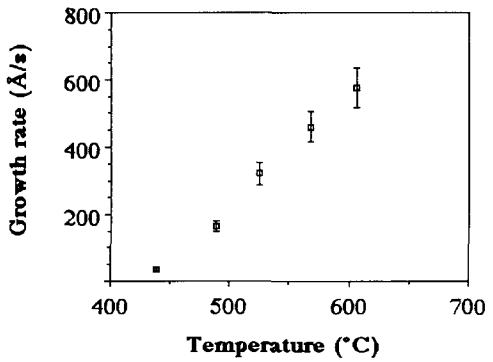

Fig. 7. Plot of growth rate as a function of temperature for films grown from 2 mol.% TMT, 4 mol.% Freon, and balance air.

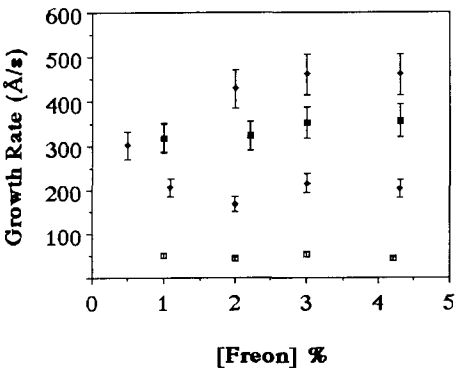

Fig. 8. Variation in growth rates for films grown at 0.1 mol.% (□), 0.5 mol.% (◆), 1 mol.% (■), and 2 mol.% (◇) TMT and balance air as a function of Freon concentration at 570 °C.

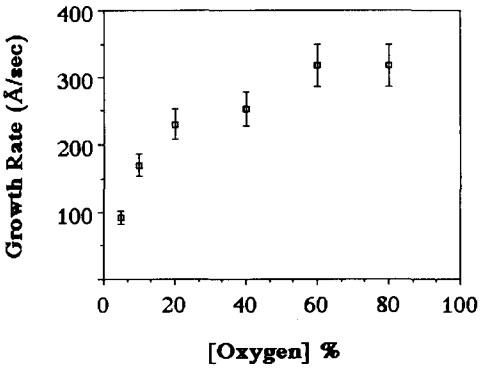

Fig. 9. Plot of the growth rate as a function of oxygen concentration for films grown at 0.5 mol.% TMT, 1 mol.% Freon, and balance air at 570 °C.

3.5. Hall effect measurements for varying temperature and reactant concentrations

The Hall mobility and carrier concentration as a function of the substrate deposition temperature are presented in Fig. 10. The mobility is observed to increase at higher temperatures indicating better film quality. It will be shown below that this trend of increasing film quality is due to the formation of larger crystallites and/or better doping efficiency at higher temperatures.

Figures 11 and 12 show the carrier concentration and Hall mobility for varying TMT and Freon concentrations for films grown at 570 °C and 610 °C. The mobility is observed to be quite high for a variety of reaction conditions with values typically between 35 and 42. These values of the mobility are among the best reported for polycrystalline doped tin oxide films. The carrier concentration is observed to be consistently low at a 0.1 mol.% TMT concentration. For films deposited at 570 °C, the carrier concentration is significantly higher at TMT concentrations of 0.5 mol.% and above, achieving values of approximately (4–6) × 10^{20} cm^{-3}.

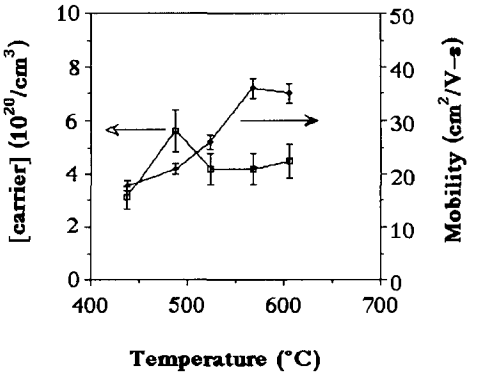

Fig. 10. Variation in carrier concentration and mobility as a function of temperature for films grown from 2 mol.% TMT, 4 mol.% Freon, and balance air.

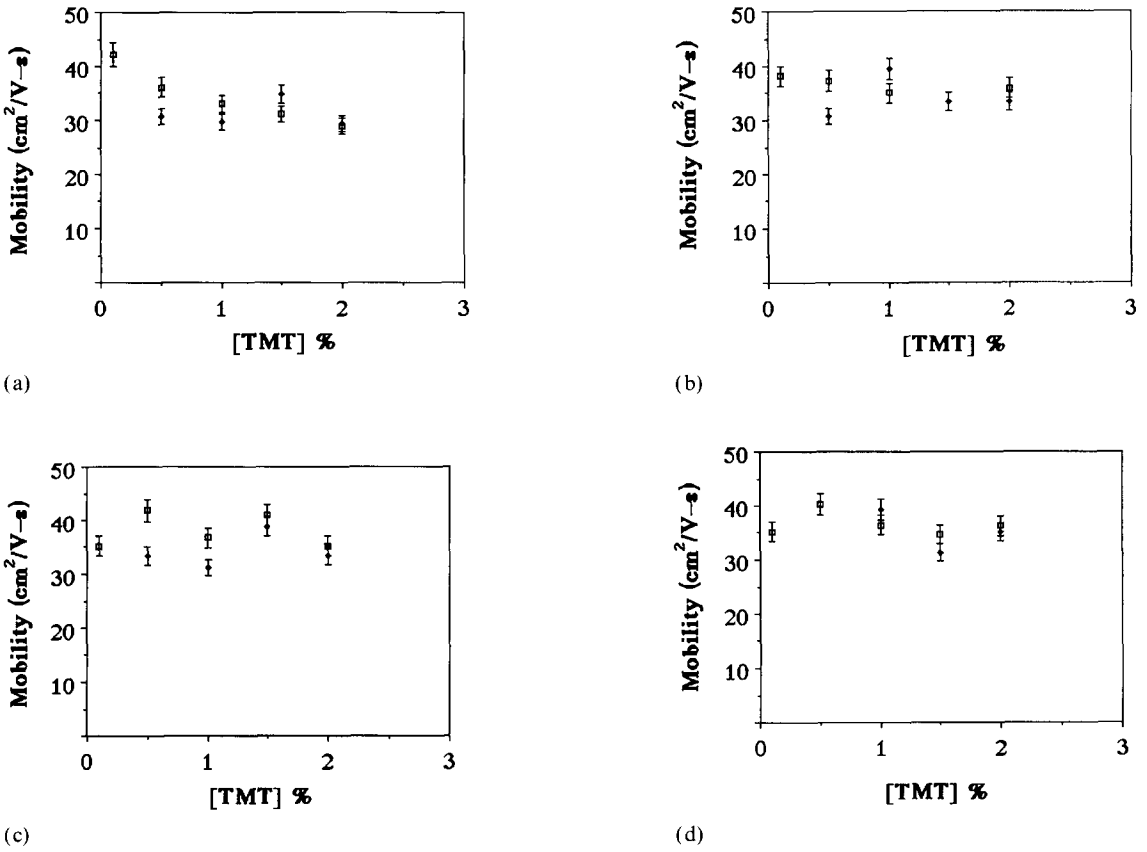

Fig. 11. Hall mobilities for films grown at (a) 1 mol.%, (b) 2 mol.%, (c) 3 mol.%, and (d) 4 mol.% Freon in air as a function of TMT concentration with deposition temperatures of 570 °C (□) and 610 °C (◆).

The combination of mobilities of 40 $cm^2 V^{-1} s^{-1}$ and carrier concentrations of about 5×10^{20} cm^{-1} translates into d.c. conductivities of nearly 3000 $\Omega^{-1} cm^{-1}$. Figure 13 plots the Hall mobility and carrier concentration at 2 mol.% TMT as a function of Freon concentration. The mobility was found to be low at 0.5 mol.% Freon (13 $cm^2 V^{-1} s^{-1}$) and increases to high values at 1–4 mol.% Freon. Similarly, the carrier concentration is low (about 1.8×10^{20} cm^{-3}) at low (0.5 mol.%) Freon concentration and becomes constant above 1 mol.% Freon. It should be stressed that carrier concentrations above 6×10^{20} cm^{-3} are not observed even if the Freon level is increased. This probably represents a solubility limit for fluorine in the tin oxide lattice (electrically inactive fluorine would not be in lattice sites).

The carrier concentration was found to decrease rapidly with increasing oxygen concentration for a series of films grown at 0.5 mol.% TMT and 1 mol.% Freon. The mobility only changes slightly for this same series (Fig. 14). The conductivity reflects this effect of the carrier concentration and decreases with increasing oxygen from a value of 2000 $\Omega^{-1} cm^{-1}$ at 20 mol.% oxygen to 300 $\Omega^{-1} cm^{-1}$ at 80 mol.% oxygen. The conductivity at higher oxygen concentration was increased to a value of 700 $\Omega^{-1} cm^{-1}$ by increasing the Freon concentration to 5 mol.%.

3.6. Doping efficiency

Figure 15 gives a plot of the fluorine atom concentration *vs.* substrate temperature. The lowest temperature in the figure (440 °C) has a lower fluorine atom concentration than the next temperature measured (490 °C). The decrease in the fluorine atom concentration at higher temperatures is consistent with chemical reaction rates leading to film deposition increasing more rapidly with temperature than the reactions which incorporate fluorine into the films. The doping efficiency is defined as the ratio of the carrier concentration to the fluorine atom concentration. This value gives the fraction of electrically active fluorine atoms incorporated into the films. The doping efficiency is observed to increase with increasing substrate temperature (also in Fig. 15). The lowest value indicates over a sevenfold excess of inactive fluorine atoms. Therefore at lower temperatures a large fraction of the fluorine atoms do not occupy the proper lattice positions to contribute to the free carrier concentration. These extra fluorine atoms may decrease the mobility and conductivity and degrade film quality.

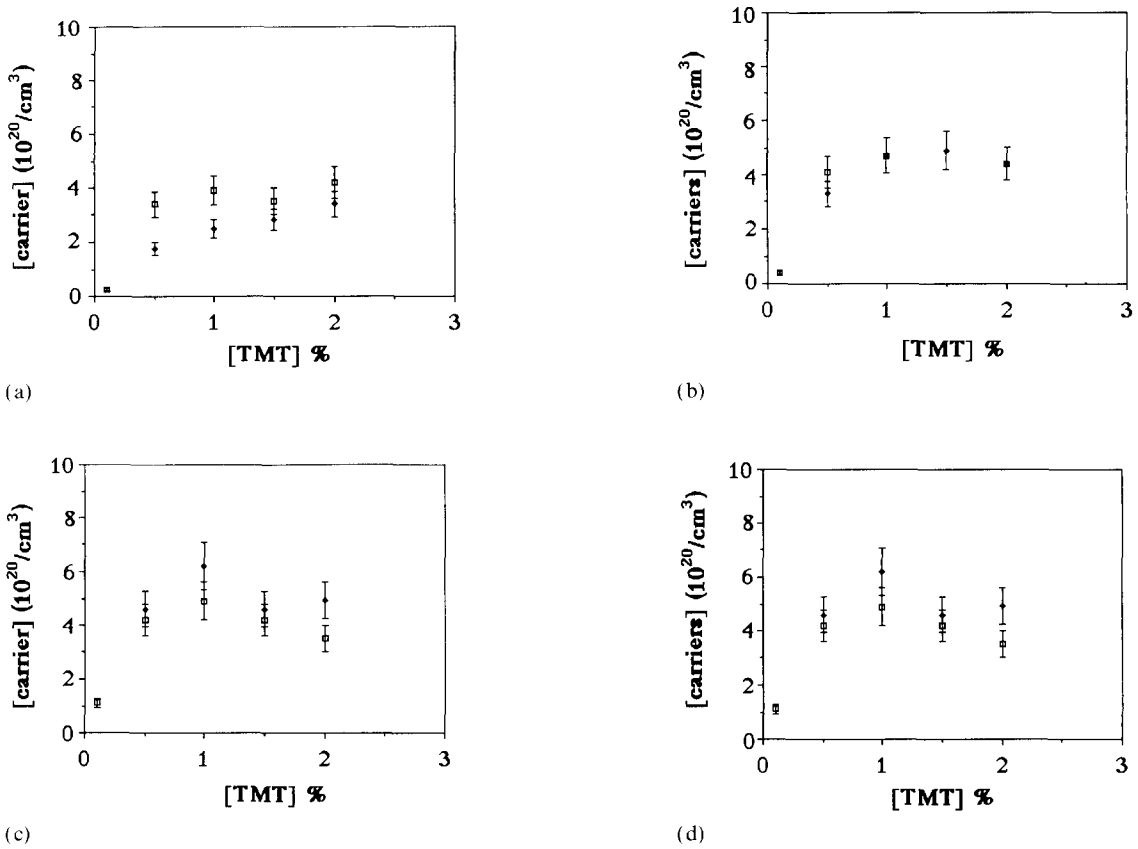

Fig. 12. Carrier concentrations for films grown at (a) 1 mol.%, (b) 2 mol.%, (c) 3 mol.%, and (d) 4 mol.% Freon in air as a function of TMT concentration with deposition temperatures of 570 °C (□) and 610 °C (◆).

This effect may partially explain the previously described increase in mobility with increasing deposition temperature. The inactive fluorine may also increase the visible absorption by introducing states in the band gap.

The fluorine atom concentration for films grown from 4 mol.% Freon in air at 570 °C is plotted in Fig. 16(a) *vs.* the concentration of TMT. Also in Fig. 16(a), the fluorine atom concentration is plotted as a function of Freon concentration with 2 mol.% TMT in air. The fluorine atom concentration is observed to increase as either the TMT or the Freon concentration increases. This is in contrast to the carrier concentration which saturates quickly as either of these concentrations is increased (Fig. 12 and 13).

In Fig. 16(b), the dependence of the doping efficiency on TMT and Freon concentration is given. At this high

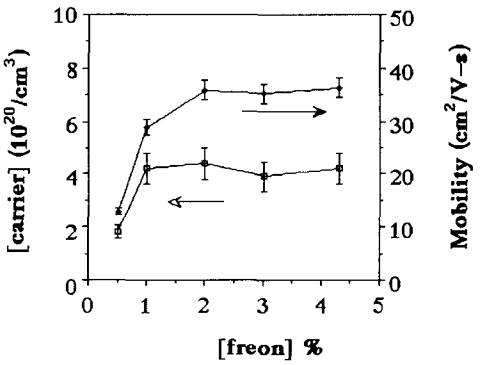

Fig. 13. Variation in carrier concentration and mobility for films grown at 2 mol.% TMT in air and 570 °C as a function of Freon concentration.

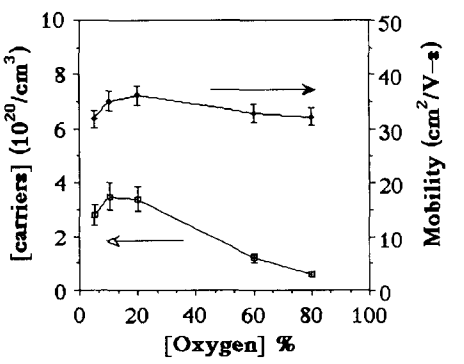

Fig. 14. Variation in carrier concentration and mobility for films grown at 0.5 mol.% TMT, 1 mol.% Freon and 570 °C as a function of oxygen concentration.

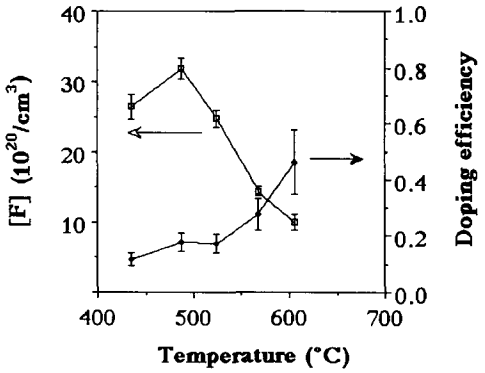

Fig. 15. Dependence of fluorine atom concentration (□) and doping efficiency (◆) on deposition temperature for films grown at 2 mol.% TMT and 4 mol.% Freon in air.

substrate temperature (570 °C), the doping efficiency approaches 100% as either the TMT or the Freon concentration is decreased.

3.7. Textured surface structure

Another important property of the tin oxide films for solar cell applications is their ability to transmit light non-specularly (diffuse transmission). For solar cell applications, this property is useful leading to the important phenomenon of light trapping [20, 21]; while for other applications such as low E window glass coating this is obviously an undesirable feature. Diffuse transmission and reflection result from the somewhat rough surfaces of the films.

Films grown at high oxgyen concentrations were observed to have rougher surface structures. SEM micrographs of films grown at 20 mol.%, 60 mol.%, and 80 mol.% oxygen, 0.5 mol.% TMT and 4 mol.% Freon (Fig. 17) reveal a pyramid-like surface structure. The surface structure is larger at the higher oxygen concentrations. Figure 18 is a plot of the diffuse transmission which shows that films grown at 40 mol.% and 60 mol.% oxygen transmit more light diffusely than the films grown at lower oxygen compositions. The diffuse transmission was fitted to the phenomenological equation

$$T_d = T_0/\lambda^n$$

where T_d is the diffuse transmission, T_0 is a parameter related to the magnitude of the scattered light (formally, it is the diffuse transmission at a wavelength of 1 μm), λ is the wavelength of light, and n describes the wavelength dependence. Values of T_0 and n were found

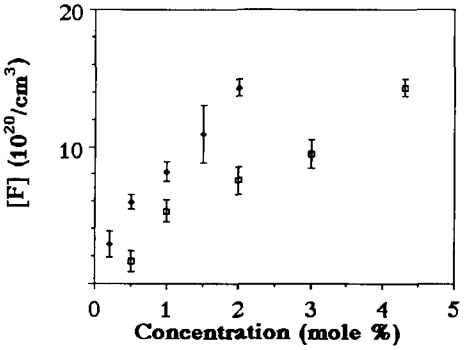

(a)

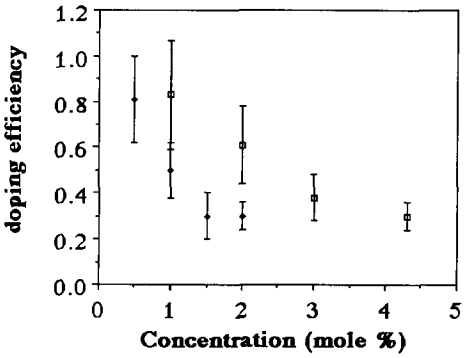

(b)

Fig. 16. (a) Variation in the fluorine atom concentration as a function of TMT (◆) at 4 mol.% Freon and balance air at 570 °C and as a function of Freon (□) at 2 mol.% TMT with balance air at 570 °C. (b) Dependence of the doping efficiency on TMT (◆) and Freon (□) concentration with balance air at 570 °C.

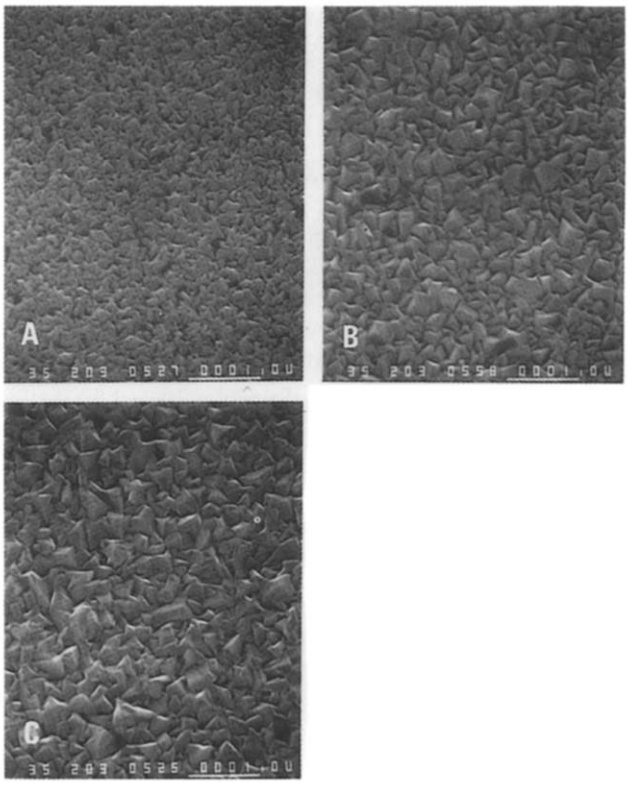

Fig. 17. SEM micrographs of films grown at (a) 20 mol.%, (b) 60 mol.%, and (c) 80 mol.% oxygen, 0.5 mol.% TMT and 1 mol.% Freon at 570 °C. (Magnifications, 20 000 ×.)

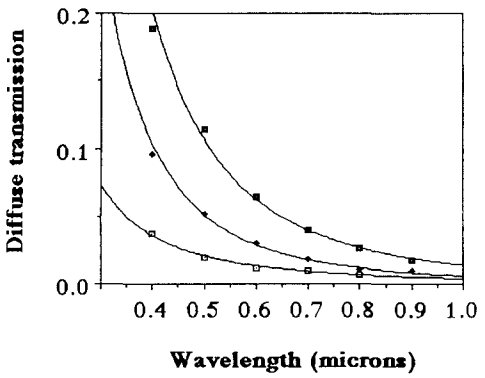

Fig. 18. Diffuse transmission for films grown at 20 mol.% (□), 40 mol.% (◆), and 60 mol.% (■) oxygen concentration and a TMT concentration of 0.5 mol.% and 1 mol.% Freon at 570 °C. The respective thicknesses are 0.91 μm with $T_0 = 0.0040$ and $n = 2.4$, 0.88 μm with $T_0 = 0.0060$ and $n = 3.1$, and 0.99 μm with $T_0 = 0.0142$ and $n = 2.9$.

by fitting the logarithm of the above equation to the experimental data. Rayleigh scattering characterized by scattering centers much smaller than the wavelength of the incident light would give a value of 4 for n. Mie scattering, with the scattering centers larger than the wavelength of light, gives a value of 2. Typically, values of n were found to be intermediate between 2 and 4 (see caption to Fig. 18).

Films grown at very low TMT concentrations of 0.1–0.5 mol.% TMT and lower oxygen concentration (about 20 mol.%) were also observed to have rough surface structures with the roughness increasing as the amount of TMT decreased. SEM of these films revealed a jagged type of surface texture. Figure 19 shows the electron micrographs of a series of films grown at 0.5–0.1 mol.% TMT and 4 mol.% Freon. We see that, as the TMT concentration is decreased, the surface becomes systematically more jagged. The structures at 0.1 and 0.2 mol.% TMT appear to be platelet like in appearance with growth preferentially in two dimensions. Figure 20 gives the diffuse transmission spectrum for films grown at TMT concentrations of 0.1 mol.%, 1 mol.%, and 2 mol.%. Consistent with the rougher surfaces observed in the SEM micrographs, the amount of diffuse scattering is much higher at the very low TMT concentrations.

It should also be mentioned that the films become somewhat more textured as the deposition temperature is increased. Figure 21 shows that the diffuse transmission increases as a function of temperature.

3.8. Crystallite orientation in the atmospheric pressure chemically vapor deposited films

Table 1 gives the X-ray diffraction patterns for films grown at increasing deposition temperatures compared with a randomly oriented powder sample. The most striking feature is that the films produced at higher temperature are highly oriented with the (200) plane parallel to the substrate, while those produced at low temperatures have (211) orientation. The widths of the X-ray peaks were used to estimate the sizes of the grains. It was found that grain size increases with increasing temperature (Fig. 22). This is most likely the major reason for the increasing film quality of this series. Previously, Goto *et al.* have found the (200) orientation to be consistent with films of excellent electrical conductivity [29]. Our results are consistent with those observations; however, it is somewhat difficult to determine separately the effect of the orientation on the electrical properties because of the concurrent increasing crystallite size and doping efficiency with increasing deposition temperature.

The X-ray diffraction analysis of the films grown from 0.3–2.0 mol.% TMT, 4 mol.% Freon, and balance air (Table 2) showed preferred orientation along the (200) plane. Likewise, films grown at 2.0 mol.% TMT and Freon concentrations varying from 1 to 4 mol.% had the same orientation. However, at a low Freon concentration of 0.5 mol.% and for no Freon the preferred orientation is different. As previously mentioned, the preferred orientation is established early in the film

TABLE 1. Relative intensity (peak height) of X-ray diffraction lines for fluorine-doped tin oxide films grown from 2 mol.% tetramethyltin and 4 mol.% Freon in air at various temperatures

Sample	Relative intensities for the following values of 2θ (corresponding diffraction lines are also given)											
	26.6° (110)	33.8° (101)	38.0° (200)	39° (111)	42.6° (210)	51.7° (211)	55° (220)	57.8° (002)	61.9° (310)	64.7° (112)	66.0° (301)	71.3° (202)
Powder	100	80	25	6	2	65	18	8	14	18	16	8
440 °C	40					100						
460 °C	55	100				62				31		
490 °C	10	72	100			9					18	
520 °C	44	35				100					32	
570 °C			100									
610 °C			100									

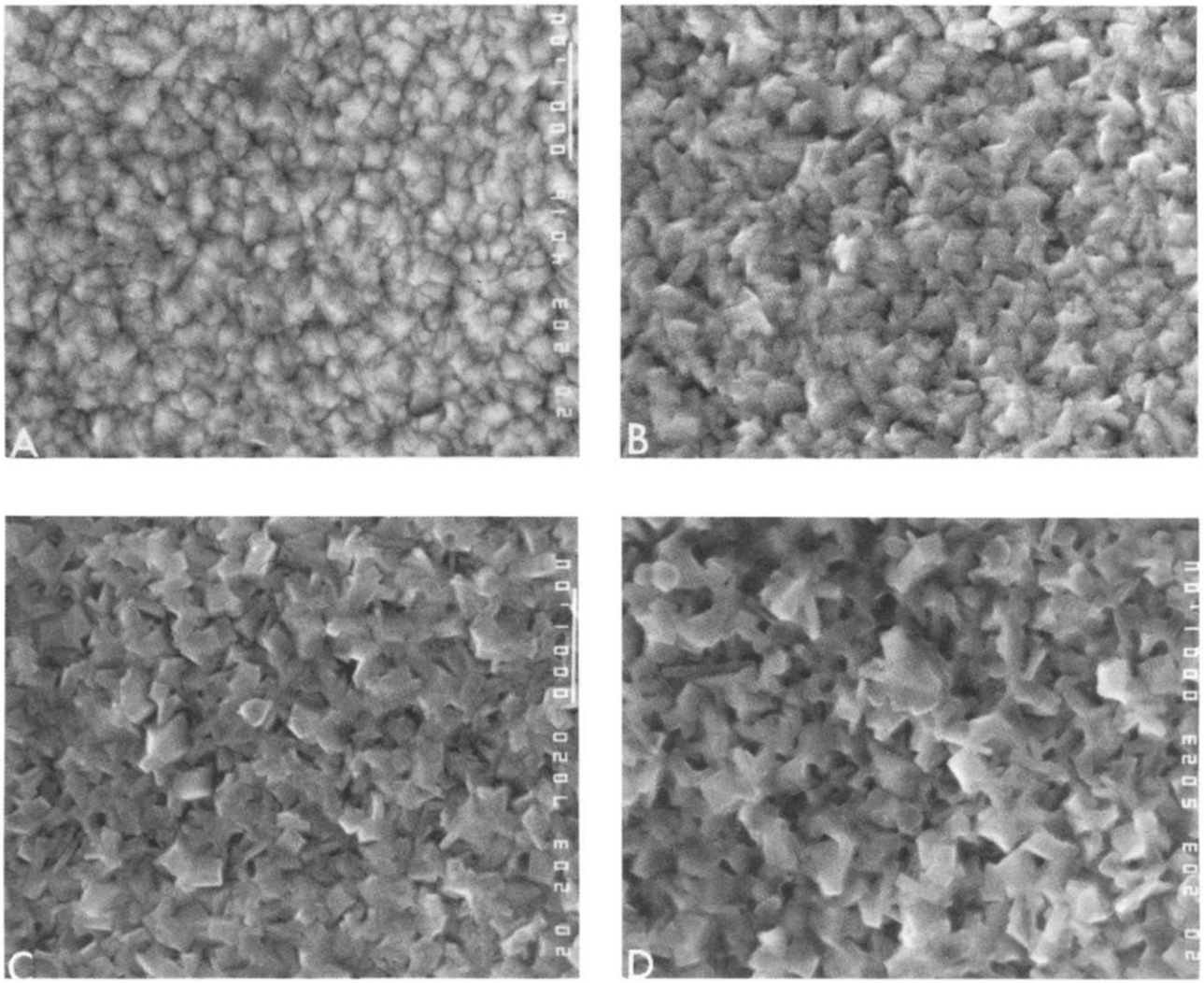

Fig. 19. SEM micrographs of films grown at (a) 0.5 mol.%, (b) 0.3 mol.% (c) 0.2 mol.%, and (d) 0.1 mol.% TMT, 4 mol.% Freon in air at 570 °C. (Magnifications, 20 000 ×.)

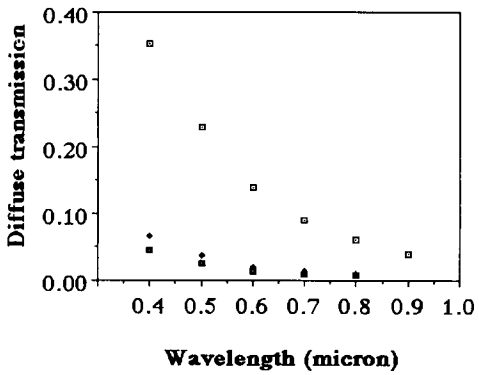

Fig. 20. Diffuse transmission for films grown at 0.1 mol.% (□), 1 mol.% (◆), and 2 mol.% (■) TMT, 4 mol.% Freon in air at 570 °C. The thicknesses are 1.21 μm, 1.01 μm, and 1.01 μm respectively.

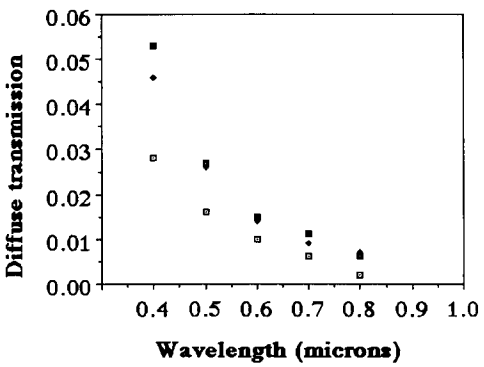

Fig. 21. Diffuse transmission for films grown at 2 mol.% TMT and 4 mol.% Freon in air as a function of deposition temperature: □, 490 °C (1.07 μm thick); ◆, 570 °C (1.01 μm); ■, 610 °C (0.86 μm).

TABLE 2. Relative intensity (peak height) of X-ray diffraction lines for fluorine-doped tin oxide films grown at 570 °C in air at various tetramethyltin and Freon concentrations

Sample	Relative intensities for the following values of 2θ (corresponding diffraction lines are also given)											
	26.6° (110)	33.8° (101)	38.0° (200)	39° (111)	42.6° (210)	51.7° (211)	55° (220)	57.8° (002)	61.9° (310)	64.7° (112)	66.0° (301)	71.3° (202)
Powder	100	80	25	6	2	65	18	8	14	18	16	8
0.3% TMT, 4% Freon			100									
0.5% TMT, 4% Freon		24	100									
1% TMT, 4% Freon	3	3	100						6			
1.5% TMT, 4% Freon		22	100									1
2% TMT, 4% Freon			100									
2% TMT, 3% Freon			100									
2% TMT, 2% Freon		1	100						1			
2% TMT, 1% Freon	4		100						2			
2% TMT, 0.5% Freon	100					7	8				2	
2% TMT, 0% Freon	85	7	11			100	7		5		70	

TABLE 3. Relative intensity (peak height) of X-ray diffraction lines for fluorine-doped tin oxide film grown at 570 °C from 0.5 mol.% tetramethyltin, 1 mol.% Freon, and 80 mol.% oxygen in air

Sample	Relative intensities for the following values of 2θ (corresponding diffraction lines are also given)											
	26.6° (110)	33.8° (101)	38.0° (200)	39° (111)	42.6° (210)	51.7° (211)	55° (220)	57.8° (002)	61.9° (310)	64.7° (112)	66.0° (301)	71.3° (202)
Powder	100	80	25	6	2	65	18	8	14	18	16	8
1% TMT, 1% Freon	100		40						24			

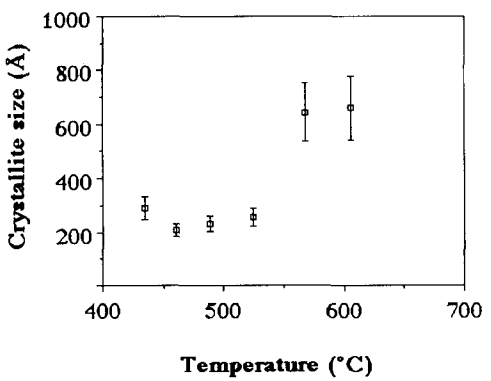

Fig. 22. Dependence of crystallite size on deposition temperature for films grown from 2 mol.% TMT and 4 mol.% Freon in air: 440 °C (0.79 μm thick), 460 °C (0.67 μm), 490 °C (0.95 μm), 520 °C (1.41 μm), 570 °C (0.92 μm), and 610 °C (0.86 μm).

deposition by at least a film thickness of 0.1 μm. The textured films grown at 0.5 mol.% TMT and 80 mol.% oxygen were found to incorporate some orientation along the (110) plane in addition to the (200) and (310) planes (Table 3).

4. Conclusions

Tin oxide films with excellent electrical and optical properties have been reproducibly deposited by the oxidation of TMT and bromotrifluoromethane. Conductivities of nearly 3000 $\Omega^{-1}\,cm^{-1}$ and Hall mobilities of up 42 $cm^2\,V^{-1}\,s^{-1}$ have been achieved. Films with these electrical properties can be produced with growth rates approaching 60 nm s^{-1}.

The films were found to be preferentially oriented in each case measured. The orientation was found to be dependent on deposition temperature, oxygen concentration, and Freon concentration. For TMT concentrations from 0.3 to 2 mol.% and Freon concentrations from 1 to 4 mol.% at a deposition temperature of 570 °C or higher the crystallites were highly oriented along the (200) direction. The crystallite sizes were larger at higher temperatures and the doping efficiency was found to increase with increasing temperature. This combined effect of larger crystallites and a lower concentration of electrically inactive fluorine atoms, which act as scattering centers, accounts for the higher mobilities achieved at higher deposition temperatures. The doping efficiency also increased for decreasing TMT or Freon concentrations. At very low TMT (below 1 mol.%) or low Freon (below 0.5 mol.%) concentrations the low carrier concentrations result in low conductivities.

Smooth tin oxide films were produced at TMT concentrations of 0.5–2 mol.% and oxygen concentrations of 5–20 mol.%. Such films are suitable as heat-reflecting coatings for window glass. Tin oxide films with rough, well-faceted surfaces were produced at 0.5 mol.% TMT and high oxygen concentrations (80 mol.%) and also at 0.1–0.3 mol.% TMT in air. These rough films are useful as transparent conductors in thin film solar cells, in which the roughness assists in light trapping [30].

Acknowledgments

This work was supported in part by the Solar Energy Research Institute (recently renamed the National Re-newable Energy Laboratory). Instruments from the Harvard Materials Research Laboratory (funded by the National Science Foundation) were used. We thank David Lange for performing the microprobe measurements.

References

1 Z. M. Jarzebski and J. P. Marton, *J. Electrochem. Soc.*, *123* (1976) 199C.
2 Z. M. Jarzebski and J. P. Marton, *J. Electrochem. Soc.*, *123* (1976) 299C.
3 Z. M. Jarzebski and J. P. Marton, *J. Electrochem. Soc.*, *123* (1976) 333C.
4 K. L. Chopra, S. Major and D. K. Pandya, *Thin Solid Films*, *102* (1983) 1.
5 J. B. Mooney and S. B. Radding, *Annu. Rev. Sci.*, *12* (1982) 81.
6 M. Fantini and I. Torriani, *Thin Solid Films*, *138* (1986) 255.
7 A. K. Abass and M. T. Mohammad, *J. Appl. Phys.*, *59* (1986) 1641.
8 F. Simonis, M. van der Leij and C. J. Hoogendoorn, *Sol. Energy Mater.*, *1* (1979) 221.
9 T. Karlsson, A. Roos and C.-G. Ribbing, *Sol. Energy Mater.*, *11* (1985) 469.
10 E. Shanthi, V. Dutta, A. Banerjee and K. L. Chopra, *J. Appl. Phys.*, *51* (1980) 6243.
11 E. Shanthi, A. Banerjee, V. Dutta and K. L. Chopra, *J. Appl. Phys.*, *53* (1982) 701.
12 H. Haitjema, J. J. Ph. Elich and C. J. Hoogendoorn, *Sol. Energy Mater.*, *18* (1989) 283.
13 Y. Takahashi and Y. Wada, *J. Electrochem. Soc.*, *137* (1990) 267.
14 A. Czapla, E. Kusior and M. Bucko, *Thin Solid Films*, *182* (1989) 15.
15 J. A. Aboaf, V. C. Marcotte and N. J. Chou, *J. Electrochem. Soc.*, *120* (1990) 267.
16 B. J. Baliga and S. K. Ghandhi, *J. Electrochem. Soc.*, *123* (1976) 941.
17 R. G. Gordon, *US Patent 4,146,657*, 1979.
18 C. G. Borman and R. G. Gordon, *J. Electrochem. Soc.*, *136* (1989) 3820.
19 G. Frank, E. Kauer, H. Kostlin and F. J. Schmitte, *Sol. Energy Mater.*, *8* (1983) 387.
20 T. Tiedje, B. Abeles, J. M. Cebulka and J. Pelz, *Appl. Phys. Lett.*, *42* (1983) 712.
21 H. W. Deckman, C. R. Wronski, H. Witzke and E. Yablonovitch, *Appl. Phys. Lett.*, *42* (1983) 968.
22 F. Jones, *Proc. R. Soc. London, Ser. A*, *166* (1938) 16.
23 F. B. Ellis and R. G. Gordon, *J. Appl. Phys.*, *54* (1983) 5381.
24 K. M. Gustin and R. G. Gordon, *J. Electron. Mater.*, *17* (1988) 509.
25 R. G. Gordon, J. Proscia, F. Ellis and S. Kurtz, *Amorphous Materials Subcontractors Review Meet.*, SERI, 1982, p. 109.
26 D. Belanger, J. P. Dodelet, B. A. Lombos and J. I. Dickson, *J. Electrochem. Soc.*, *132* (1985) 1398.
27 K. H. Kim and J. S. Chun, *Thin Solid Films*, *141* (1986) 287.
28 D. Strickler, *PhD Thesis*, Harvard University, 1989.
29 Y. Goto *et al. Jpn. Patent Sho 60-65073*, 1986.
30 R. G. Gordon, J. Proscia, F. B. Ellis, Jr., and A. E. Delahoy, *Sol. Energy Mater.*, *18* (1989) 263.